Available online at www.sciencedirect.com
ScienceDirect
Journal of Power Sources 176 (2008) 207–214
JOURNAL OF POWER SOURCES
www.elsevier.com/locate/jpowsour

Development and characterization of a miniature PEM fuel cell stack with carbon bipolar plates

Po-Chang Lin [1], Benjamin Y. Park *, Marc J. Madou [1]

Department of Mechanical & Aerospace Engineering, 4200 Engineering Gateway Building, University of California, Irvine, CA 92697, USA

Received 20 September 2007; received in revised form 16 October 2007; accepted 17 October 2007
Available online 1 November 2007

Abstract

This paper details the fabrication and testing of a fuel cell stack using a novel manufacturing approach for creating carbon bipolar plates. The fundamental fabrication techniques have been described in a previous contribution [1]. The initial paper characterized a single cell. In this work, the fabrication techniques are utilized to fabricate a three-cell fuel cell stack. Operating data in different operating conditions is measured and presented. Information on cell performance at different operating temperatures and pressures is included. The methodology for the fuel cell characterization is presented.

Keywords: Fuel cell; Bipolar plate; Carbon; C-MEMS; Miniature; Characterization

1. Introduction

Electronic devices are becoming smaller, lighter, and more multi-functional. With the trend of devices becoming smaller and more portable, the volume and weight of the battery contributes to a major portion of the product. As predicted, battery technology has quickly become the bottleneck of portable device development. The power demand for a typical microprocessor has increased by the factor of 80 in 10 years. In contrast, battery capacity has only increased by a factor of three. Battery capacity has not kept up with the tremendous rate of increasing power consumption of integrated circuit (IC) technology (Moore's Law). This has forced manufacturers to search for alternative solutions. Fuel cells are seen by many as a future alternative to batteries for mobile applications. Today, many companies (Motorola, NEC, Casio, Toshiba, Fuji, Intel, MTI, ISE, Polyfuel. . .etc.) are developing miniature fuel cells as battery replacements for various consumer and military electronic devices [2]. Because of the fuel storage issue, most of them use methanol in either direct methanol fuel cells or through micro-reformers in regular PEM fuel cells [3,4]. Because the output voltage of a single unit cell within a fuel cell is typically less than 1 V, multiple cells are often configured in series into a fuel cell stack. A significant part of the PEMFC fuel cell stack is the bipolar plate, which can account for about 80% of the total weight and 45% of stack cost [5]. In this contribution, we will describe the fabrication of fuel cell stacks using bipolar plates made by carbonization of machined polymer sheets.

2. Experimental/materials and methods

2.1. Carbon microelectromechanical systems

Carbon microelectromechanical systems, or C-MEMS, describe a manufacturing technique in which carbon devices are made by treating a pre-patterned organic structure at high temperatures in an inert or reducing environment. Today, C-MEMS provides a material and microfabrication solution to creating micro-carbon structures for use in many applications including batteries and fuel cells.

The C-MEMS process is shown in Fig. 1. The specific raw organic material is machined or patterned into the structure that is desired. The pyrolysis process is carried out in a closed ceramic tubular furnace in vacuum or a forming gas (95% N_2

* Corresponding author. Tel.: +1 949 824 6585; fax: +1 949 824 8585.
E-mail addresses: violin0707@yahoo.com.tw (P.-C. Lin), bypark@uci.edu (B.Y. Park), mmadou@uci.edu (M.J. Madou).
[1] Tel.: +1 949 824 6585; fax: +1 949 824 8585.

0378-7753/$ – see front matter © 2007 Elsevier B.V. All rights reserved.
doi:10.1016/j.jpowsour.2007.10.079

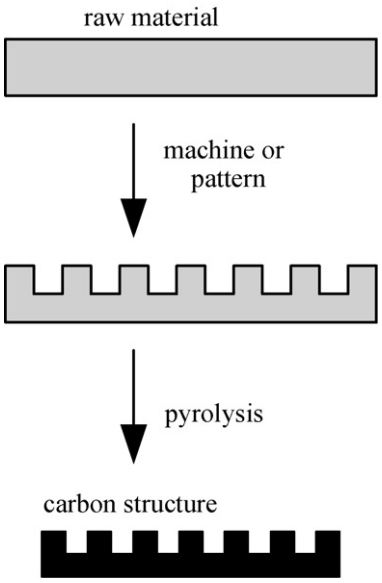

Fig. 1. The C-MEMS process.

and 5% H_2) atmosphere at around 900 °C. The whole structure is converted into carbon through this process.

By changing the pyrolysis time, temperature and process profile, structures having different shapes, conductivity, and mechanical properties can be fabricated. In the current case, the C-MEMS technique is used to replace the graphite machining that is commonly used for fabricating bipolar plates [6].

Making bipolar plates using C-MEMS technology has the following benefits:

(1) Resistance to corrosion: The bipolar plates are exposed to an extremely corrosive environment inside of a fuel cell stack, which is usually at a pH of 2–3 [2]. Carbon can withstand this severe environment unlike most metals.
(2) Material homogeneity: The bipolar plate, gas diffusion layer, and catalyst support layer are all made of carbon. This means robustness can be increased and electrical resistance can be reduced.
(3) Easy to machine: Bipolar plates made of directly machined graphite are difficult to fabricate and expensive because the material is extremely brittle. The raw material is easy to machine in the process described in this paper. The manufacturing cost can be reduced.
(4) Reduced weight and size: Compared with directly-machined graphite or molded graphite plates which are porous and need to be thick [2,6], smaller and thinner bipolar plates can be fabricated. Lighter and smaller fuel cells can be made. In this study, C-MEMS-based bipolar plates have been successfully fabricated and integrated into a fuel cell stack.

2.2. Fuel cell test station

A test station was set up to operate and test the fuel cells. The fuel cell test system consists of several components: an air compressor, a hydrogen tank, humidifiers, regulators, gauges, and flow meters. The entire experiment setup is shown in Fig. 2.

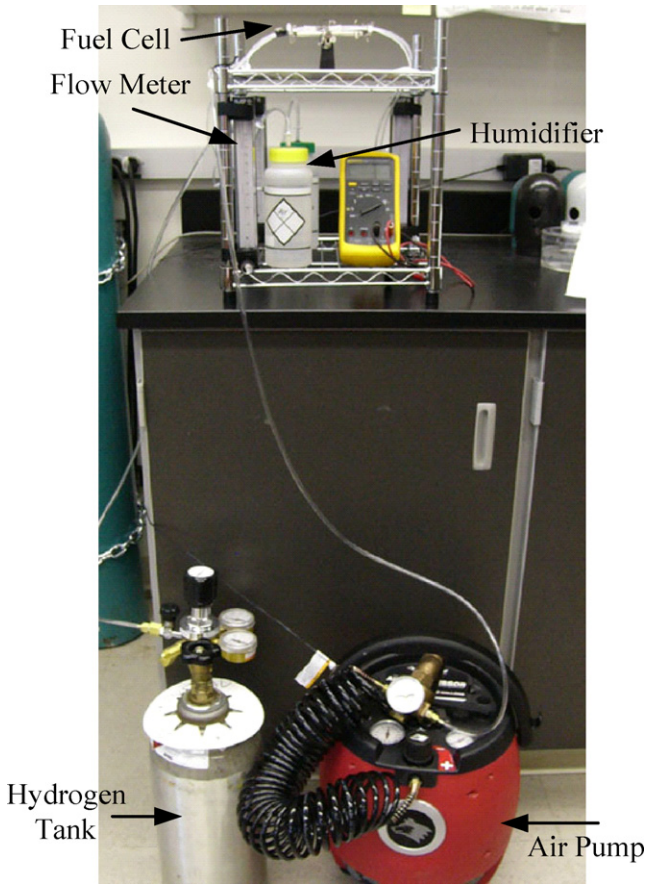

Fig. 2. The fuel cell test station.

2.3. PEM fuel cell component fabrication and integration

2.3.1. Design features

In Fig. 3, a schematic of the PEM fuel cell stack is shown. The developed stack has screw holes on each bipolar plate corner to align all the components. Another benefit of using

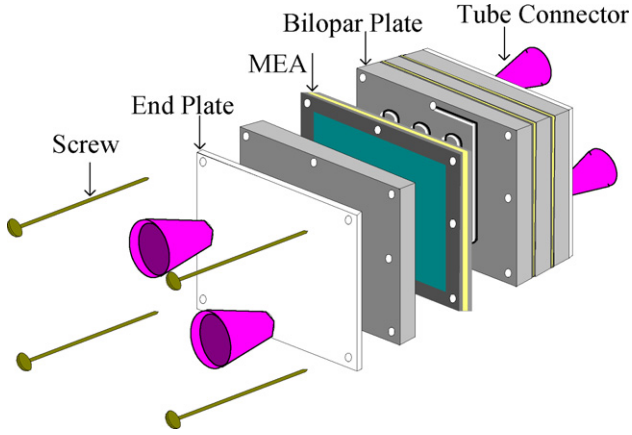

Fig. 3. The fuel cell stack configuration.

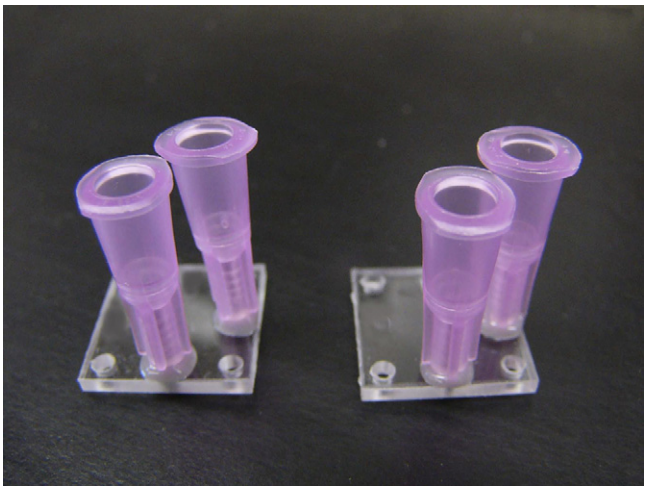

Fig. 4. End plates.

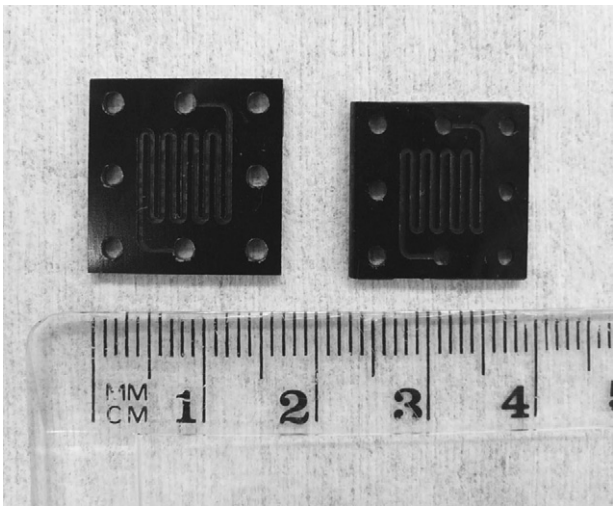

Fig. 5. Bipolar plates (left: before carbonization, right: after carbonization).

a screw hole is better control of compression pressure while stacking the cells [3].

2.3.2. Fuel cell components and manufacturing

2.3.2.1. End plate. The end plates serve as the interface between the fuel cell stack and other subsystems (the gas supply and the electrical circuit). The end plates are made of plastic and were machined in a circuit board milling tool (T-Tech – Norcross, GA) to create the holes and gas inlet/outlet ports. The connectors, the purple parts in Fig. 4, are cut from conventional 16 G (1.291 mm diameter) syringe tips.

2.3.2.2. Bipolar plate. In miniature fuel cells, the channel size is an important parameter [7]. It was shown that small channels have advantages over designs with large channel sizes [8,9], such as higher flow velocity that helps preventing flooding and less dead zones (area where no reaction occurs). However, once the channels become too small, water can accumulated and the pressure drops can be too large. Moreover, channels need to be large enough to machine. Depending on the geometry of the design, the optimal channel size was found to be 100 μm in one study [9] and approximately 500 μm in another [10]. A serpentine channel [11] which has a size of 500 μm was used in the present study.

Kapton® is available as very thin films and not applicable for our use. For miniature fuel cell applications, a thicker material must be used. Cirlex® is a Dupont product made by bonding multiple thin layers of Kapton® using adhesive-less bonding technology. A 60-mil (1.524 mm) thick Cirlex® (Fralock – Canoga Park, California) sheet was chosen as the raw material for making the bipolar plates. It was machined with 500 μm diameter end mills in a circuit board milling tool (T-Tech – Norcross, GA) to create the fluidics on both sides. A serpentine flow pattern was used. Four screw holes were made on each corner for alignment purposes, and four inlet/outlet holes for gases were created on each side of the square. The original size of the bipolar plate was 1.8 cm × 1.8 cm. The polymer plate shrank to a size of 1.45 cm × 1.45 cm after carbonization. The bipolar plates were heated up within a nitrogen atmosphere from room temperature to 300 °C in 30 min. The temperature was kept constant at 300 °C for 1 h. The furnace was then heated up to 900 °C (2 h). The atmosphere was changed from nitrogen to forming gas and the samples were heat-treated at 900 °C for 1 h. The samples were cooled to 700 °C (1 h) then room temperature (3 h) in a nitrogen atmosphere. The shrinkage was ∼20% and the average electrical resistance of the bipolar plates was 30 ohms (from one plane to the other). Fig. 5 shows the shrinkage of the bipolar plates after carbonization.

2.3.2.3. Gasket. The gaskets are placed between the each electrolyte and bipolar plate. The gasket not only needs to be elastic to prevent gas leakage and support, but also has to be durable and corrosion resistant. The gasket also needs to be very thin (almost as thin as the electrode which is made of carbon paper) but robust. After several tests, a thin silicone rubber film was chosen. The 0.01 in. (254 μm) silicone rubber film was cut using a Graphtec CE2000-60 plotter. The gaskets are shown in Fig. 6.

2.3.2.4. Membrane electrode assembly (MEA).

2.3.2.4.1. Membrane. A Nafion® 115 sheet (purchased from Electrochem – Woburn, MA) is used as the electrolyte. The sheet was cut into pieces using the Graphtec CE2000-60 plotter before activation. Because Nafion® will swell to ∼110% of its original size after hydration, it was cut into a smaller size, 1.3 cm × 1.3 cm. The sheets expanded to 1.45 cm × 1.45 cm after hydration/activation. The Nafion® was activated by a series of heated baths [12,13]. It was submersed in 80 °C DI water for 1 h, followed by a 1-h 80 °C 30% hydrogen peroxide bath, and then another 1 h 80 °C bath in 10 M sulfuric acid (1:1 dilution of pure H_2SO_4 and DI water). Finally, a short rinse in DI water is performed and the membrane is stored in DI water before fabrication of the MEA.

2.3.2.4.2. Electrodes. Anode and cathode electrodes for a fuel cell consist of catalyst ink loaded onto a gas diffusion backing [14,15]. Gas diffuses through the backing and is broken down by catalysts [16–19]. Commercial electrodes were used (EC-20-10-7, Electrochem – Woburn, MA). The carbon sup-

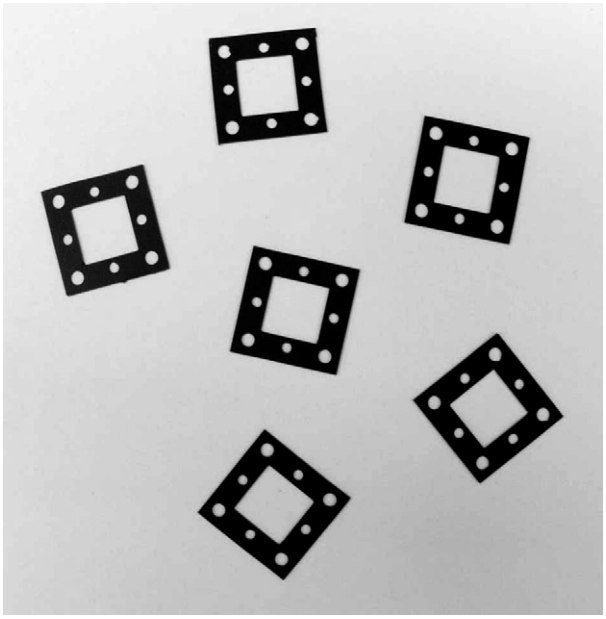

Fig. 6. Completed gaskets.

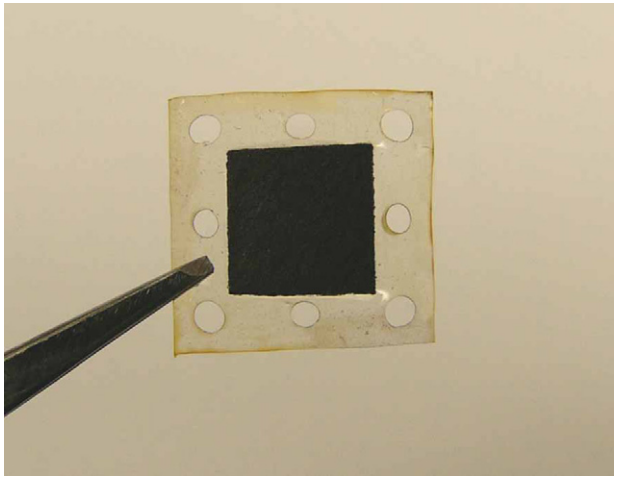

Fig. 7. A photo of a finished membrane electrode assembly (MEA).

ported catalyst layer had a 1 mg cm^{-2} Pt loading with 20 wt.% Pt/Vulcan XC-72. To fabricate a Direct Methanol Fuel Cell, all that is needed to be done is the replacement of the anode electrode with a Pt/Ru catalyst loaded electrode [20]. The electrode sheet was cut into the size of the final area, 0.8 cm × 0.8 cm, and brushed with 5% Nafion® solution (EC-NS-05-250 ml, Electrochem – Woburn, MA). The Nafion® solution coated electrodes were placed in a dry and cool environment at room temperature until dry.

2.3.2.4.3. Assembly. To make the MEA, the following procedure was used: the electrodes were placed on either side of the membrane and pressed into the membrane sheet. Two metal

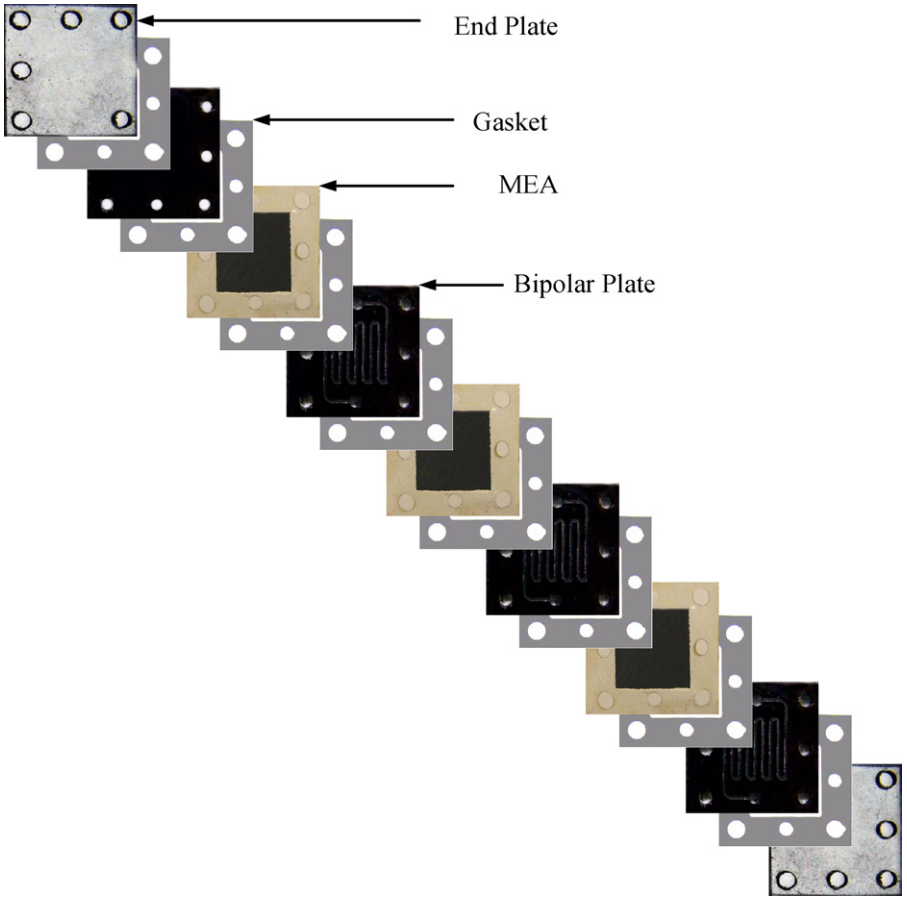

Fig. 8. Configuration of a three-cell fuel cell stack.

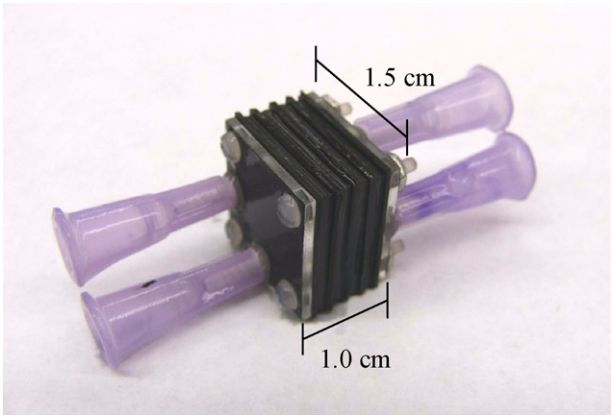

Fig. 9. A photo of an assembled three-cell fuel cell stack.

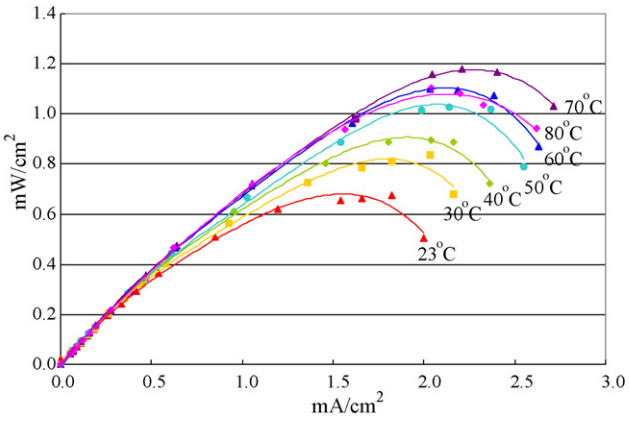

Fig. 11. Effect of operating temperature on the fuel cell power curve.

plates were used to hold the electrodes and membrane in place, and a C-clamp was used to hold and supply sufficient pressure on the whole structure. The MEA was heated while pressed from room temperature to 90 °C in 1 h and then ramped to 130 °C in 30 min. The C-clamp is tightened and left at 130 °C for 5 min. A glass container of water was placed inside of the heating environment and a water soaked fabric was also used to cover the MEA in order to prevent drying out of the membrane. Fig. 7 shows a finished membrane electrode assembly (MEA).

2.3.3. Integration of a fuel cell stack

The stack is stacked in the order of: end plate, rubber gasket, bipolar end plate, rubber gasket, MEA, rubber gasket, bipolar plate, rubber gasket . . . and end plate, which is depicted in Fig. 8. The final assembled fuel cell stack is shown in Fig. 9.

Since the bipolar plates shrink after pyrolysis and the electrolyte swells up after hydration, good dimension control is essential to ensure that the components are compatible during assembly.

3. Fuel cell test and analysis

3.1. Effect of operating temperature

Single cells were tested under different operating temperatures. Figs. 10 and 11 show the results of a series of experiments in which the operating temperature was gradually increased from room temperature (23 °C) to 80 °C in 10 degree steps, and the resulting polarization curves clearly show voltage gain with increased temperature. However, we can see a performance drop at the temperature of 80 °C. The performance drop is most likely due to dehydration of the membrane.

3.2. Effect of operating pressure

Single fuel cells were tested under different operating pressures. In this experiment, the hydrogen pressure was fixed at 3 psi (20.68 kPa), and the pressure of air was gradually increased from 3 psi (20.68 kPa) to 10 psi (68.95 kPa). Figs. 12 and 13 show the results of this series of experiments and the resulting polarization curves clearly show voltage gain with increased air pressure. However, The pressure effect is not as significant as the temperature effect. The output voltage gain is only ∼30 mV even when the inlet air pressure was more than tripled from 3 psi (20.68 kPa) to 10 psi (68.95 kPa). Higher gas pressure helps remove the water in the flow channel and prevents flooding [21]. Unlike the temperature effect, the slope of the polarization curve does not change significantly.

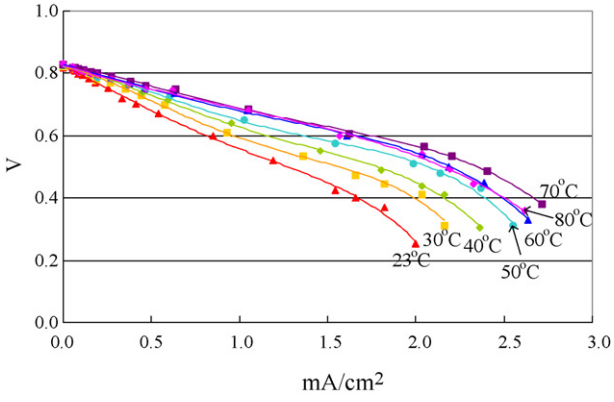

Fig. 10. Effect of operating temperature on the fuel cell polarization curve.

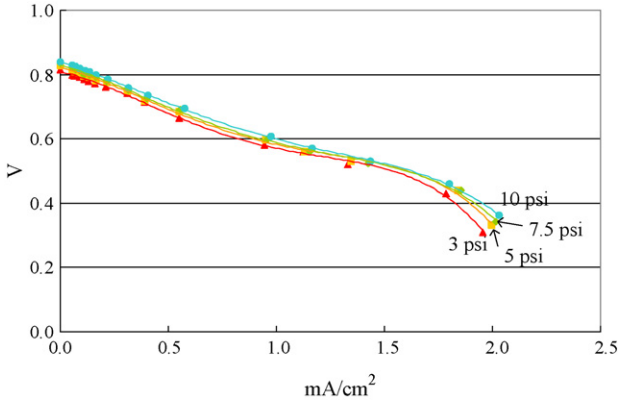

Fig. 12. Effect of operating pressure on the fuel cell polarization curve.

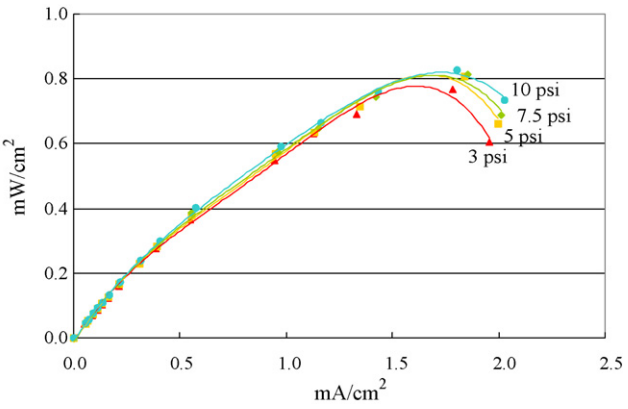

Fig. 13. Effect of operating pressure on the fuel cell power curve.

Table 1
EIS test parameters

Initial frequency (Hz)	10^5
Final frequency (Hz)	0.01
Points/decade	5
AC voltage (mV)	10
Area (cm^2)	0.64

Table 2
Fuel cell stack operating condition

Temperature	24 °C
Air pressure	30 psi (206.84 kPa)
H_2 pressure	30 psi (206.84 kPa)
Air flow rate	19.6 sccm (0.018 g min^{-1})
H_2 flow rate	20 sccm (0.025 g min^{-1})

3.3. Electrical impedance spectroscopy (EIS) analysis

A series of PEM fuel cell EIS tests were carried out using a GAMRY® cell test station at different operating voltages ranging from open circuit to 0.38 V. The Nyquist plots for each operating point are shown in Fig. 14. The Nyquist plots provide useful polarization information on the major component interfaces. The parameters that were used in the test are listed in Table 1:

This result shows that the fuel cell resistance is relatively high and that there are several improvements that can be made. The impedances associated with the electrode–electrolyte interface were relatively large. The estimated resistance in the cathode electrode–electrolyte interface is 280 ohm-cm^2. Further investigation on triple phase boundary, including electrode structures and catalyst layers, will be carried out in the future.

3.4. The three-cell PEM fuel cell stack

The fuel cell stack was composed of three cells in series. The active area of each electrode was ~0.64 cm^2. The operating conditions are listed in Table 2:

The characterization results are shown in Figs. 15 and 16. The open circuit voltage was ~0.8 V for a single cell and 2.3 V for the three-layer fuel cell stack. The polarization curve of each single cell was measured before they were connected

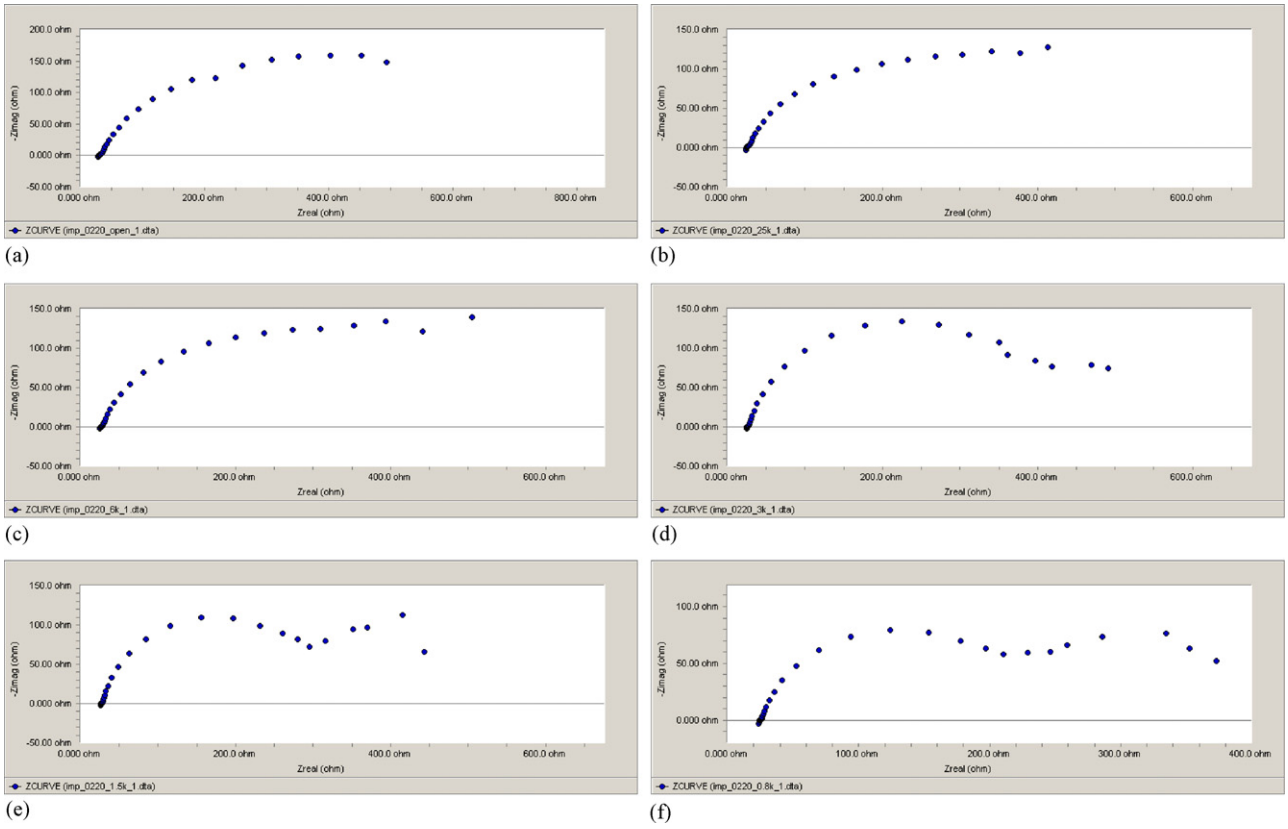

Fig. 14. The Nyquist plots of a single cell at different operating points: (a) open circuit, (b) 0.73 V, (c) 0.67 V, (d) 0.593 V, (e) 0.48 V, (f) 0.38 V.

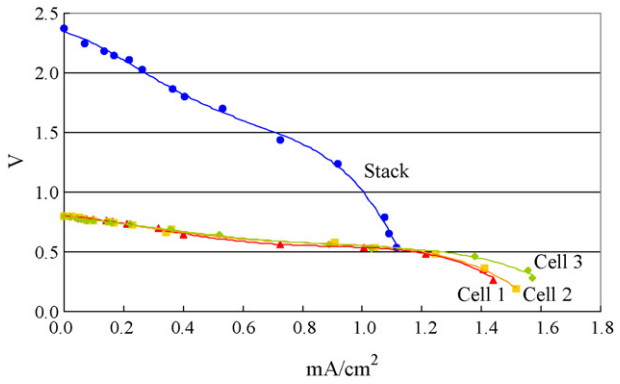

Fig. 15. Polarization curve of the fuel cell stack and single cells.

in series. In the current–potential curves, the three-cell stack shows a much steeper slope reaching the mass transfer polarization region earlier than that of the single cells. The two different kinds of curves (stack and single cell) are separated by a large potential difference in the beginning but reach the same potential around 1.1 mA cm^{-2}. However, the three-cell stack always has a much larger power density, compared to a single cell before reaching the mass-transfer polarization region.

Listed below are some conclusions from the testing of the fuel cell stack:

(1) Increasing the total number of cells in a stack requires higher pressure and flow rate than single cells in order to have sufficient gas distribution. However, high pressure and high flow rates could cause drying problems and requires extra energy. Thus, stack and flow pattern design is extremely important and these parameters effect stack performance dramatically.
(2) Increasing the total number of cells in the PEMFC stack increases the mass-transfer impedance proportionally [22].
(3) Increasing the total number of cells shows a steeper slope in the potential–current curve than that of the single cell case.
(4) Increasing the total number of cells does increase the overall power density. The three-cell stack power output was triple that of a single cell before the mass-transfer polarization region.

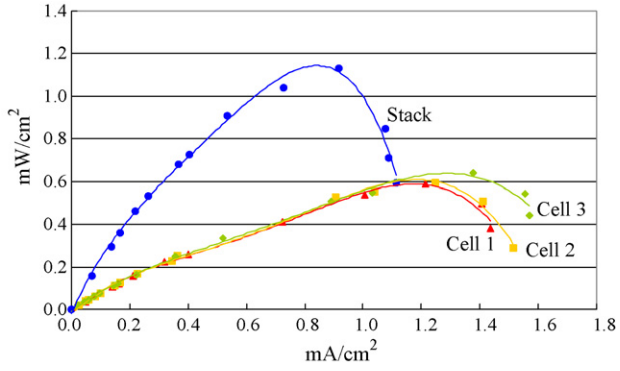

Fig. 16. Power curve of the fuel cell stack and single cells.

(5) For a fuel cell stack, humidity is much more important than single cells. The mass-transfer impedance varies considerably as humidity changes. With a decrease in humidity, a mass transfer impedance increase was observed.
(6) Fuel cell stack integration and operation is much more challenging compared to single cells due to several aspects: even gas/humidity/temperature distribution, sealing problems, and compression force through the whole structure.

4. Conclusions

A miniature C-MEMS based PEM fuel cell stack with an active area of 0.64 cm^2 (per cell) has been developed and its electrochemical properties have been characterized. The C-MEMS technology has demonstrated capability to provide a flexible venue of fabrication for miniature fuel cells with a complex flow field. The fabricated bipolar plates are based on a polymer material called Cirlex®, and the MEA was made of Nafion® 115 and catalyst coated carbon electrodes. The three-cell PEM fuel cell stack demonstrated a maximum power density of 1.18 mW cm^{-2} at room temperature using hydrogen and air under 30 psi (206.84 kPa). The advantage of easy manufacturing makes this type of miniature PEM fuel cell stack well suited to power future portable electronics and MEMS devices.

The optimum operating temperature for the presented design is around 60–80 °C with external humidification. Cell performance increased when pressure was increased but the extent is far less than the temperature effect. It is not energy efficient to enhance the performance by increasing the operating pressure unless the pressure comes from an already pressurized source. In order to have better gas distribution in a fuel cell stack, the pressure cannot be too low or the mass-transfer polarization lowers the overall cell voltage.

Electrical impedance spectroscopy (EIS) results show that the fuel cell resistance is relatively high and that there are several improvements that can be made. The major contributor to this high impedance is the large resistance of the electrode–electrolyte interfaces.

Further cell performance improvement will be carried out in the near future. These studies will investigate in detail and optimize the following: electrode structure, catalyst ink, MEA manufacturing, scaling effects and water management.

Acknowledgements

The authors gratefully acknowledge all the C-MEMS team members in the Madou group. We thank Professor G. Scott Samuelsen and Dr. Jack Brouwer in the National Fuel Cell Research Center (NFCRC) for their discussion and comments. Finally, the authors appreciate the support of the research through a sponsored research agreement by Carbon Micro Battery, LLC.

References

[1] B.Y. Park, M.J. Madou, J. Power Sources 162 (2006) 369–379.
[2] F. Barbir, PEM Fuel Cells Theory and Practice, second ed., Elsevier, Burlington, 2001, pp.15–16, 101–102, 117–120.
[3] J. Larminie, A. Dicks, Fuel Cell Systems Explained, second ed., Wiley, Chichester, 2003, pp. 6–9, 34–37, 141–142.
[4] X. Ren, T.E. Springer, T.A. Zawodzinski, S. Gottesfeld, J. Electrochem. Soc. 147 (2000) 466–474.
[5] A. Hermann, T. Chaudhuri, P. Spagnol, Int. J. Hydrogen Energy 30 (2005) 1297–1302.
[6] H.S. Lee, W.S. Chu, Y.C. Kang, H.J. Kang, S.H. Ahn, ICCES 4 (3) (2007) 195–200.
[7] J.P. Meyers, H.L. Maynard, J. Power Sources 109 (2002) 76–88.
[8] S. W. Cha, S. J. Lee, Y. I. Park, F. B. Prinz, "Investigation of Transport Phenomena in Micro Flow Channels for Miniature Fuel Cells", 2003 Proceeding of the 1st International Conference on Fuel Cell Science, Engineering and Technology, Rochester, New York, April 21–23, 2003, Article 1171.
[9] S.W. Cha, R. O'Hayre, S.J. Lee, Y. Saito, F.B. Prinz, J. Electrochem. Soc. 151 (2004) A1856–A1864.
[10] S.W. Cha, R. O'Hayre, Y. Saito, F.B. Prinz, J. Power Sources 134 (2004) 57–71.
[11] X. Li, I. Sabir, J. Hydrogen Energy 30 (2005) 359–371.
[12] J. Kim, S.M. Lee, S. Srinivasan, C.E. Chamberlin, J. Electrochem. Soc. 142 (1995) 2670–2674.
[13] Y.W. Rho, O.A. Velev, S. Srinivasan, Y.T. Kho, J. Electrochem. Soc. 142 (1994) 2084.
[14] J. Pettersson, B. Ramsey, D. Harrison, J. Power Sources 157 (2006) 28–34.
[15] E. Antolini, Mater. Chem. Phys. 78 (2003) 563–573.
[16] S. Litster, G. McLean, J. Power Sources 130 (2004) 61–76.
[17] B. Wang, J. Power Sources 152 (2005) 1–15.
[18] V. Artero, M. Fontecave, Coordin. Chem. Rev. 249 (2005) 1518–1535.
[19] T.V. Nguyen, J. Electrochem. Soc. 143 (1996) L103–L105.
[20] H. Liu, C. Song, L. Zhang, J. Zhang, H. Wang, D.P. Wilkinson, J. Power Sources 155 (2006) 95–110.
[21] J. Zhang, R. Shimoi, K. Shinohara, D. Kramer, E. Lehmann, G.G. Scherer, Book of Abstracts 14th International Conference on the Properties of Water and Steam in Kyoto, Japan, August 29–September 3, 2004.
[22] Z. Qi, A. Kaufman, J. Power Sources 109 (2002) 469–476.